

Submitted:
16.02.2023
Accepted:
11.04.2023
Published:
23.08.2023

Ultrasound of the palmar aspect of the hand: normal anatomy and clinical applications of intrinsic muscles imaging

Riccardo Picasso¹, Federico Zaottini¹, Federico Pistoia¹,
Maribel Miguel Perez², Marta Macciò³, Deborah Bianco³, Simone Rinaldi³,
Michelle Pansecchi³, Gabriele Rossi³, Luca Tovt³, Carlo Martinoli^{1,3}

¹ Department of Radiology, IRCCS Policlinico San Martino, Genoa, Italy

² Unit of Human Anatomy and Embryology, Department of Pathology and Experimental Therapeutics, Faculty of Medicine and Health Sciences, University of Barcelona, Hospitalet de Llobrega, L'Hospitalet de Llobrega, Spain

³ Department of Health Sciences (DISSAL), University of Genoa, Genoa, Italy

Corresponding author: Federico Zaottini; e-mail: federico.zaottini.fz@gmail.com

DOI: 10.15557/JoU.2023.0021

Keywords

hand imaging;
ultrasound;
thenar;
hypothenar;
lumbricals

Abstract

Intrinsic hand muscles play a fundamental role in tuning the fine motricity of the hand and may be affected by several pathologic conditions, including traumatic injuries, atrophic changes induced by denervation, and space-occupying masses. Modern hand surgery techniques allow to target several hand muscle pathologies and, as a direct consequence, requests for hand imaging now carry increasingly complex diagnostic questions. The progressive refinement of ultrasound technology and the current availability of high and ultra-high frequency linear transducers that allow the investigation of intrinsic hand muscles and tendons with incomparable resolution have made this modality an essential tool for the evaluation of pathological processes involving these tiny structures. Indeed, intrinsic hand muscles lie in a superficial position and are amenable to investigation by means of transducers with frequency bands superior to 20 MHz, offering clear advantages in terms of resolution and costs compared to magnetic resonance imaging. In addition, ultrasound allows to perform dynamic maneuvers that can critically enhance its diagnostic power, by examining the questioned structure during stress tests that simulate the conditions eliciting clinical symptoms. The present article aims to review the anatomy, the ultrasound scanning technique, and the clinical application of thenar, hypothenar, lumbricals and interossei muscles imaging, also showing some examples of pathology involving these structures.

Introduction

Recent advances in hand surgery have led to the development of targeted minimally invasive interventions that allow treatment of a variety of pathologic conditions involving small and complex structures, including intrinsic muscles⁽¹⁾. As a direct consequence, the number of requests for hand imaging has reached unprecedented levels and these often carry diagnostic questions the answers to which implicate specific expertise with extensive knowledge of regional anatomy and hand biomechanics. Moreover, competences that spread into several fields of medical sciences such as radiology, orthopedics, and rheumatology, are essential for an expert in hand imaging, as the diagnostic accuracy is significantly increased when the radiological evaluation follows a comprehensive clinical exam. The progressive refinement of ultrasound (US) technology and the current availability of high and ultra-high frequency linear transducers that allow the investiga-

tion of intrinsic hand muscles and tendons with incomparable resolution have made this modality an essential tool for the evaluation of pathological processes involving these tiny structures⁽²⁾. Indeed, intrinsic hand muscles lie in a superficial position and are amenable to investigation by means of transducers with frequency bands superior to 20 MHz, offering clear advantages in terms of resolution and costs compared to magnetic resonance imaging (MRI). In addition, US allows to perform dynamic maneuvers that can critically enhance its diagnostic power, by examining the questioned structure during stress tests that simulate the conditions eliciting clinical symptoms. Furthermore, sonography can provide guidance to diagnostic aspirations, biopsies, and therapeutic interventions. The present article aims to review the anatomy and the US scanning technique of the volar hand with a special focus on intrinsic muscles, also presenting explanatory cases of pathologies where information provided by US significantly impacted the clinical management of patients.

Thenar muscles

Four muscles are found in the bulk of the thenar eminence, and their function is to coordinate the fine movements of the thumb (Fig. 1 A and B)⁽³⁾. The abductor pollicis brevis (APB) is the most superficial and radial muscle and, through its action, shifts the thumb anteriorly along an axis perpendicular to the palm. It is a flat and small muscle innervated by the recurrent motor branch (RMB) of the median nerve, which arises from the flexor retinaculum, the scaphoid tubercle, and in some cases, from the tubercle of the trapezium, and inserts on the base of the first phalanx of the thumb, the capsule of the metacarpophalangeal joint, and the lateral sesamoid. The flexor pollicis brevis (FPB) is composed of a superficial and deep belly located on the ulnar side of APB, and through its contraction, it flexes the proximal phalanx of the thumb on the first metacarpal and flexes and internally rotates the first metacarpal on the trapezium. The superficial belly is usually innervated by RMB and originates from the distal part of the flexor retinaculum and the tubercle of the trapezium, whereas the deep belly in most instances is at least partially supplied by the motor branch of the ulnar nerve (MBUN) and arises from the trapezoid and the capitate. Both heads distally converge with APB and insert into the radial side of the base of the proximal phalanx embedding the lateral sesamoid. The opponens pollicis (OP) is a small triangular muscle lying deep to APB and lateral to FPB. It originates from the flexor retinaculum and the tubercle of the trapezium and inserts into the whole length of the metacarpal bone

of the thumb on its radial side. It is usually supplied by RMB and through its action contributes to opposing the thumb to the palm by flexing the first carpometacarpal joint. The adductor pollicis (AddP) consists of an oblique and a transverse head, both innervated by MBUN and whose primary actions are to adduct the first metacarpal and extend the thumb interphalangeal joint. The oblique head arises from the capitate, the bases of the second and third metacarpals, the volar intercarpal ligaments, and the sheath of the flexor carpi radialis tendon, whereas the transverse head has a broad origin from the diaphysis of the third metacarpal. The two heads converge and insert on the ulnar base of the proximal phalanx of the thumb, embedding the medial sesamoid. Some fibers from the oblique head are redirected dorsally and inserted into the extensor hood of the thumb. Placing the probe perpendicular to the long axis of the first metacarpal, the four muscles of the thenar eminence are easily included in one single image, forming three distinct layers around the tendon of the flexor pollicis longus (Fig. 1 C). The first layer is composed from radial to ulnar side by APB and the superficial belly of FPB. The second layer is located on the same plane of the flexor pollicis longus tendon and only includes OP. The third layer is located deep to the tendon and consists of the deep belly of FPB and AddP. Atrophic changes affecting the thenar muscles are found in several conditions, including carpal tunnel syndrome, motor neuron diseases, polyneuropathies, and iatrogenic injury to RMB^(4,5). In addition, due to the high functional demand of the thumb, the thenar muscles may be exposed to distraction traumas, which more often involve APB and

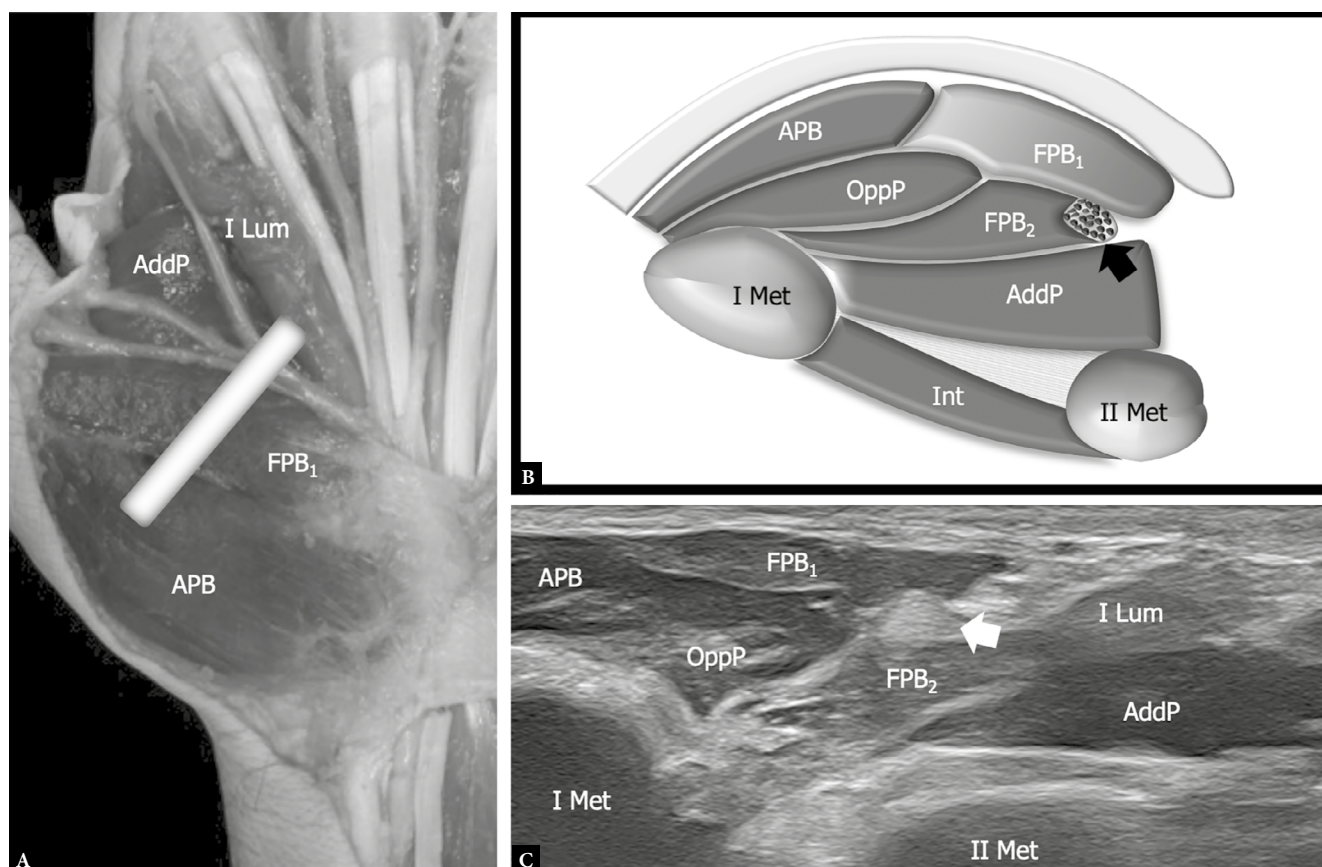


Fig. 1. Thenar eminence anatomy. Anatomic dissection, schematic drawing, and oblique 18–5 MHz US image demonstrate the normal anatomy of the thenar eminence muscles. APB – abductor pollicis brevis; FPB₁ – the superficial belly of the flexor pollicis brevis; FPB₂ – the deep belly of the flexor pollicis brevis; AddP – adductor pollicis; OppP – opponens pollicis; Int – I dorsal interosseous; I Met – I metacarpal; II Met – II metacarpal; I lum – I lumbrical muscle; arrow – flexor pollicis longus tendon. The bar in A indicates the position of the probe in C

OP (Fig. 2)⁽⁶⁾. Finally, several neoplastic and non-neoplastic lesions may be found around the thenar eminence⁽⁷⁾. US may provide essential information on the nature of the mass through the analysis of its echotexture, compressibility, and vasculature and the identification of ancillary findings, including pedicles of origin in the case of ganglia and continuity of the mass with a peripheral nerve in the case of neurogenic tumors (Fig. 3)⁽⁸⁾. In any case, when doubts on the nature of the lesion persist, the information provided by US must be integrated with high-resolution MRI data and histological analysis.

Hypothenar muscles

The hypothenar eminence includes three muscles innervated by MBUN that control part of the motricity of the little finger (Fig. 4 A and B)⁽⁹⁾. The abductor digiti minimi (ADM) is the most ulnar

muscle and arises from the pisiform bone, the flexor retinaculum, and the pisohamate ligament. Its distal tendon may embed a sesamoid before inserting into the ulnar side of the proximal phalanx, the palmar plate of the fifth metacarpophalangeal joint, and through a dorsally located slip, the extensor apparatus. The main function of ADM is to abduct the fifth metacarpophalangeal joint but, through its dorsal attachment, it assists the fourth lumbrical and the third ventral interosseous in flexing the metacarpophalangeal joint while extending the proximal interphalangeal joint. The flexor digiti minimi (FDM) is located on the radial side of ADM and originates from the hamate hook, the flexor retinaculum, and the radial aspect of the pisiform. Of note, the proximal insertion of ADM and FDM delimits a narrow passageway through which MBUN reaches the deep part of the palm which has been referred to as the pisohamate hiatus. In most instances, FDM blends distally with ADM tendon and inserts into the medial aspect of the base of the proximal phalanx, but sev-

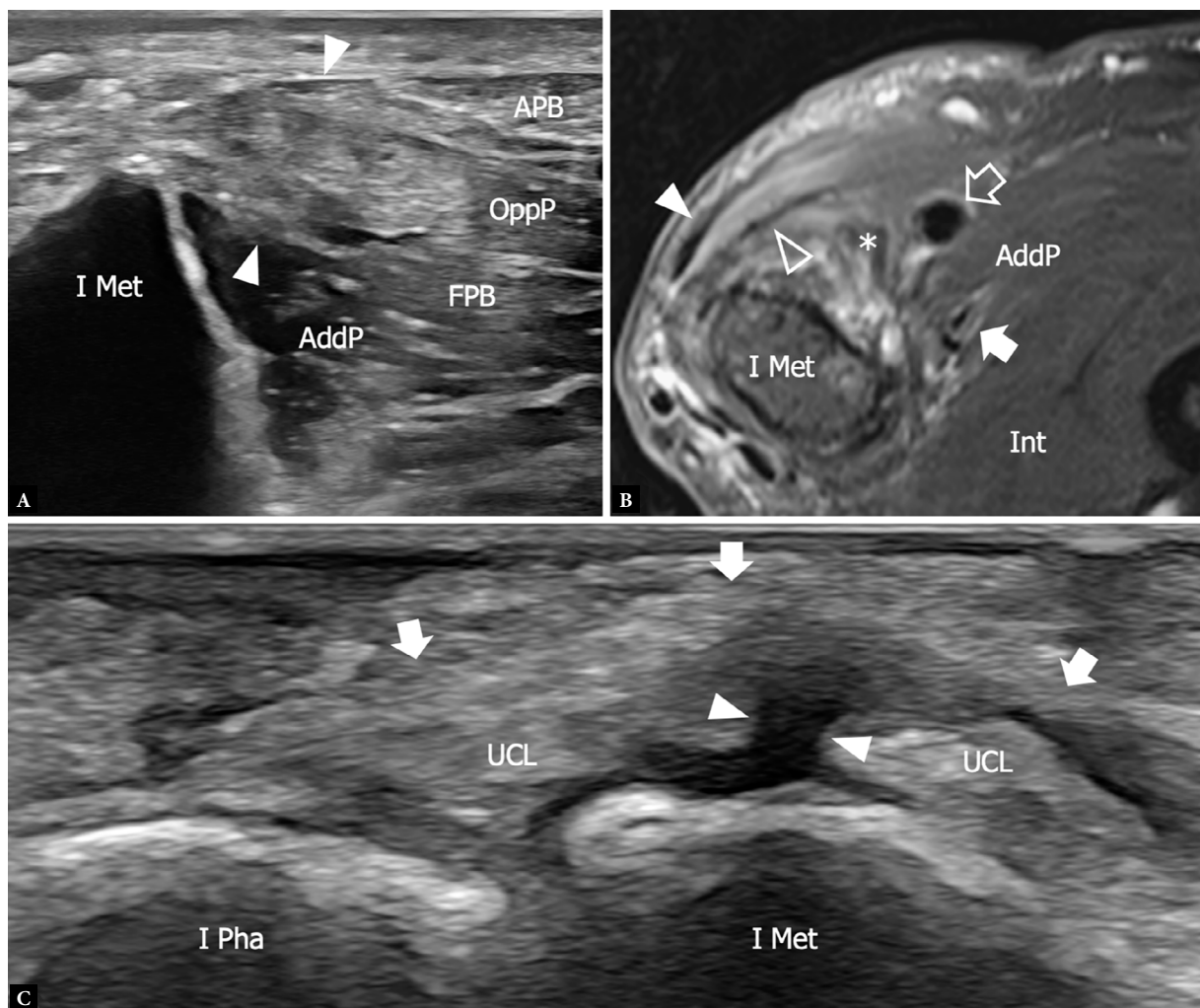


Fig. 2. Strain injury of the thenar muscles in a patient with distraction trauma of the first metacarpophalangeal joint. **A.** Short-axis 22–8 MHz US image obtained at the level of the first metacarpal neck demonstrates edematous changes with muscle hyperechogenicity (arrowheads) affecting the abductor pollicis brevis (APB), the opponens pollicis (OppP), and the most radial fibers of the flexor pollicis brevis (FPB), corresponding to a grade I distraction injury. **B.** Correlative transverse oblique tSE T2-weighted MRI with fat saturation shows high signal intensity corresponding to edema at the distal myotendinous junction of the abductor pollicis brevis (arrowhead) and opponens pollicis (outlined arrowhead). Note mild edema of the flexor pollicis brevis (asterisk) and minor strain of the intramuscular aponeurosis of the adductor pollicis (arrow). Outlined arrow, flexor pollicis longus tendon; Int, first dorsal interosseous muscle. **C.** Long-axis 22–8 MHz US image shows a full thickness tear (arrowhead) of the ulnar collateral ligament of the first metacarpophalangeal joint (UCL). The torn ligament maintains its regular position underneath the adductor aponeurosis (arrows), so the patient was managed conservatively. I Pha – first phalanx; I Met – first metacarpala

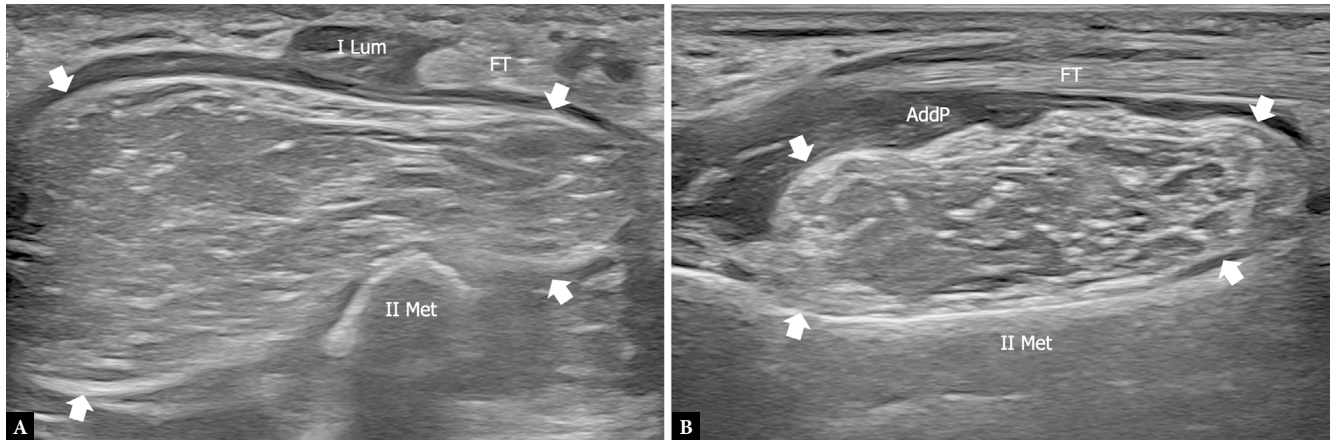


Fig. 3. Intramuscular lipoma in a patient with a progressively enlarging lump at the thenar eminence. **A.** Transverse and **B.** Longitudinal 22–8 MHz US images demonstrate a large hyperechoic lesion (arrow) located inside the muscle belly of the adductor pollicis (AddP). The mass lies over the bony cortex of the II metacarpal and dislocates superficially the flexor tendons for the index (FT) and the first lumbrical muscle (I Lum). Note the striated echotexture characteristic of lipomatous tumor. Histologic analysis confirmed a well-differentiated lipoma and the patient was managed conservatively

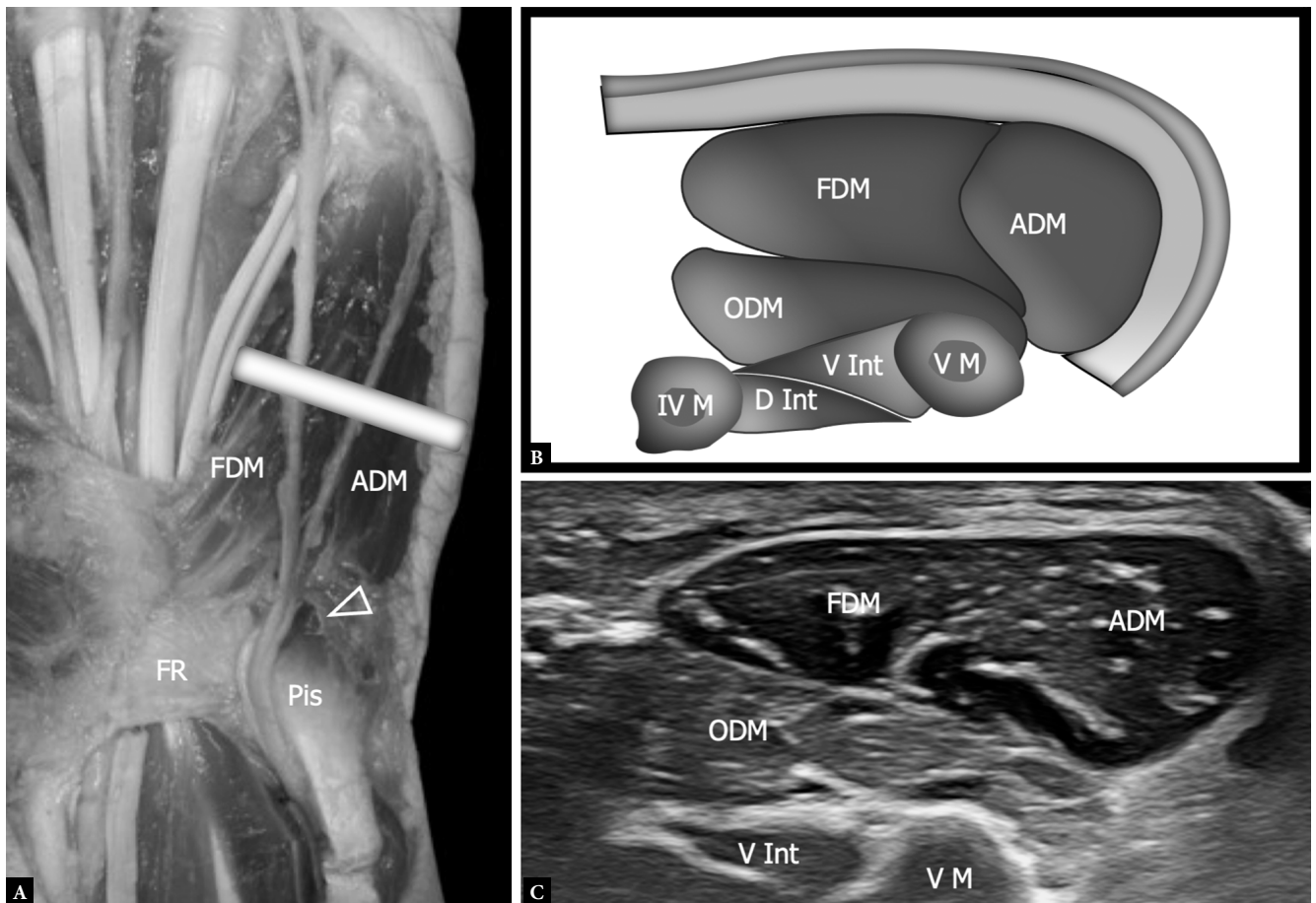


Fig. 4. Hypothenar eminence anatomy. Anatomic dissection, schematic drawing, and oblique 18-5MHz US image demonstrate the normal anatomy of the hypothenar muscles. ADM – abductor digiti minimi; FDM – flexor digiti minimi; ODM – opponens digiti minimi; V int – third ventral interosseous; D Int – fourth dorsal interosseous; FR – flexor retinaculum; Pis – pisiform; outlined arrowhead – pisohamate hiatus; IV Met – fourth metacarpal; V Met – fifth metacarpal. The bar in **A** indicates the position of the probe in **C**

eral anatomical variances have also been described, including the absence of FDM with concurrent hypertrophy of ADM or independent FDM insertion into the fifth metacarpal head⁽¹⁰⁾. The primary function of FDM is to flex the fifth metacarpophalangeal joint. The

opponens digiti minimi (ODM) lies deep to ADM and FDM, originates from the hamate hook and the flexor retinaculum, and inserts into the ulnar aspect of the fifth metacarpal shaft. The ODM flexes and laterally rotates the fifth metacarpals over the fifth carpometa-

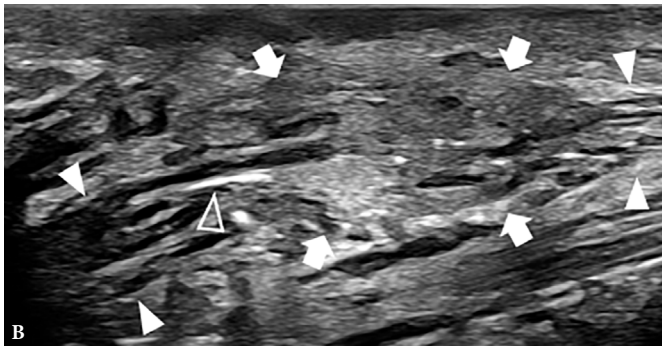
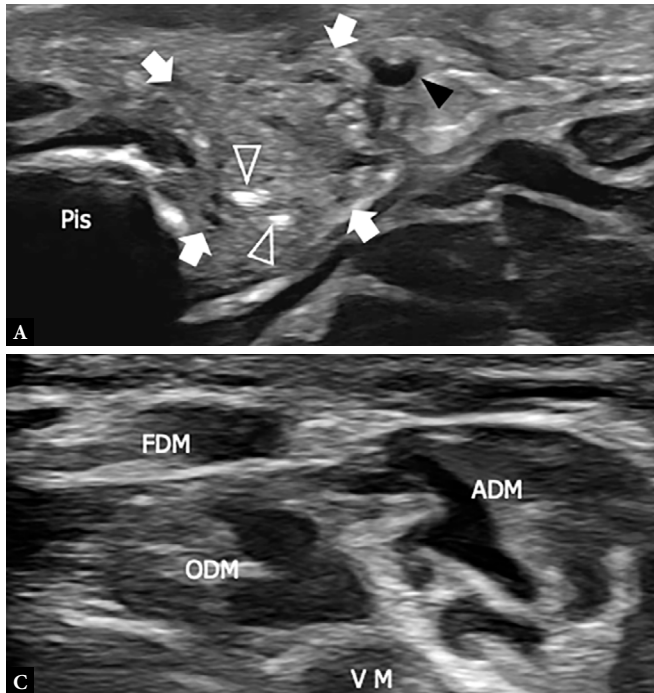


Fig. 5. Hypothenar muscle wasting in a patient with right ulnar nerve neurotmesis repaired through epineurial suture. **A.** Transverse and **B.** Longitudinal 22–8 MHz US image obtained at the level of the proximal Guyon tunnel demonstrates a hypertrophic intraneural scar (arrows) located inside the ulnar nerve (white arrowhead), with loss of the fascicular echotexture and derangement of the axons. Note the suture (outlined arrowhead) inside the nerve. These findings should be interpreted as a failure in nerve healing with the development of a neuroma-in-continuity. Pis – pisiform; black arrowhead – ulnar artery. **C.** Transverse 18–5MHz US image demonstrated atrophy of the Abductor (ADM) Opponens (ODM) and Flexor (FDM) digiti minimi. VM, fifth metacarpal

carpal joint, bringing the little finger in opposition to the thumb. The hypothenar muscles are easily identified by orienting the probe in the short axis of the fifth metacarpal shaft, where they appear situated in two distinct layers (Fig. 4 C). ADM and FDM compose the superficial layer and are respectively located on the ulnar and radial sides of the metacarpal shaft. ODM is located deep to the previous two muscles in close relationship with the fifth metacarpal, where it inserts. The palmaris brevis (PB) is a thin superficial muscle that sits in the subcutaneous tissue of the hypothenar eminence. It arises from the transverse carpal ligament and from the palmar aponeurosis and inserts into the skin. Even if the main PB function is to protect the ulnar nerve and the ulnar artery from blunt traumas over the ulnar aspect of the palm, it also plays a minor role in tensing the skin of the hypothenar during grip action⁽¹¹⁾. Hypothenar muscle atrophic changes are commonly found in cubital tunnel syndrome, or when the ulnar nerve is damaged at the Guyon canal proximal to its bifurcation (Fig. 5)⁽¹²⁾. Partial involvement or complete sparing of the hypothenar muscles may happen in cases where MBUN is damaged distal to the level of origin of the motor branches for a specific muscle. Generally speaking, ADM and FDM branches originate from UNMB proximal to the level of the pisohamate hiatus and consequently, selective atrophy of ODM may occur when the nerve is compressed distal to this level⁽¹³⁾. Even if strain injuries of the hypothenar muscles have not been reported, they may be involved by compression trauma in the so-called hammer syndrome⁽¹⁴⁾. Finally, space occupying masses may develop inside hypothenar muscles (Fig. 6). The differential diagnosis of these entities follows the same principles described in the previous paragraph for thenar muscles.

Lumbricals

Four lumbricals are found in the intermetacarpal spaces⁽¹⁵⁾. The two radial lumbricals are respectively innervated by the proper volar digital nerve for the radial side of the index finger and the first common digital nerve, whereas the ulnar lumbricals are supplied by the

MBUN. Generally speaking, the lumbricals arise in the palm from the tendon slips for the second to the fifth fingers of the flexor digitorum profundus (FDP), move into the dorsal compartment distal to the level of the deep transverse intermetacarpal ligament, and insert into the radial part of the extensor hood of the same finger, but they may also send some fibers to the volar plate or to the base of the proximal phalanx (Fig. 7 A). More in detail, the insertion point on the extensor hood may be the lateral band, the Landsmeer ligament, or the transverse fibers. As for the proximal origin, lumbrical muscles consistently originate from the radial side of the FDP tendons for the second, third, fourth, and fifth finger around the level of the carpal tunnel outlet, but some variance exists. Indeed, recent anatomic work found that whereas the first lumbrical is a unipennate muscle that only arises from the radial side of the FDP tendon for the index finger, the second and third lumbricals may also have accessory origins from the ulnar side of the adjacent tendons in 21% and 36% of cases, respectively⁽¹⁵⁾. The fourth lumbrical was found to be the most variable, having a bipennate origin from the opposite sides of the FDP tendons for the fourth and fifth fingers in most cases (57%) and a unipennate origin from the ulnar side of the FDP tendon for the fourth finger in 14% of people. In a minority of cases, the second, third, and fourth lumbricals may also originate from the muscle belly of the adjacent lumbrical muscles. Due to their small dimensions, the lumbricals are better evaluated by means of US probes with frequency bands around 20 MHz (Fig. 7 B and C). The probe should be placed in the mid palm oriented in the short axis of the metacarpal shafts. The lumbricals are demonstrated in the intermetacarpal spaces between the flexor tendons. Whereas the first lumbrical is easily appreciated along its whole length until the distal insertion, the second, third, and fourth lumbricals are only partially amenable to US distal to the deep intermetacarpal ligament due to their deep location in between the metacarpal heads. The main function of lumbricals is to flex the metacarpophalangeal joints while extending the interphalangeals. Lumbricals are biomechanically prone to distraction injuries due to their unique anatomic configuration, characterized by proximal and distal inser-

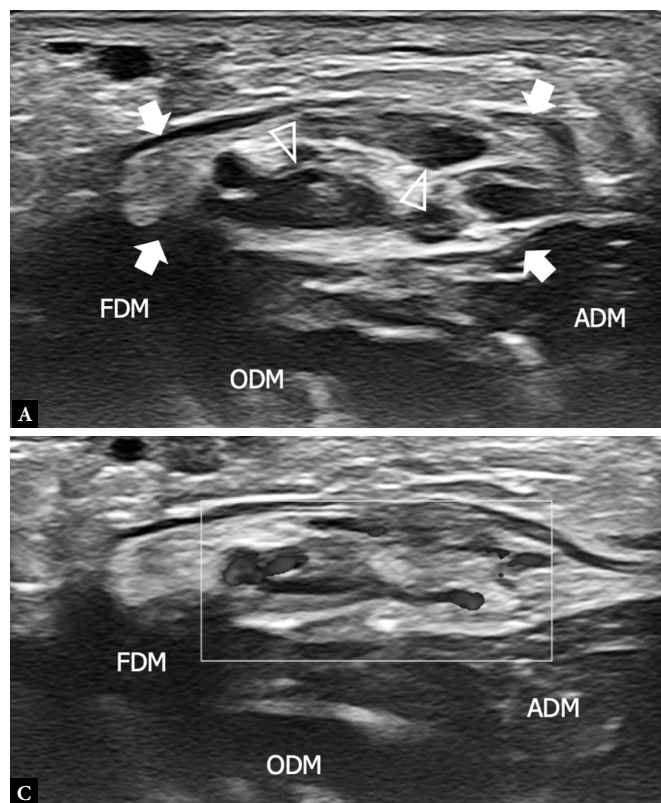


Fig. 6. Intramuscular arteriovenous malformation in a patient with a soft lump at the level of the hypothenar eminence. **A, B.** Short-axis 24–8 MHz US images obtained at the level of the hypothenar eminence, **A** with and **B** without exerting compression of the soft tissue with the probe, respectively, demonstrate a compressible mass (arrows) with a mixed echotexture consisting of ectasic and convoluted vascular structures (outlined arrowheads) surrounded by a hyperechoic matrix. The mass is located inside the muscle bellies of the abductor (ADM) and flexor (FDM) digiti minimi, whereas the opponens (ODM) is spared. **C.** Short-axis 24–8 MHz doppler image shows flow signals inside the convoluted vessels. These findings are consistent with an arteriovenous malformation

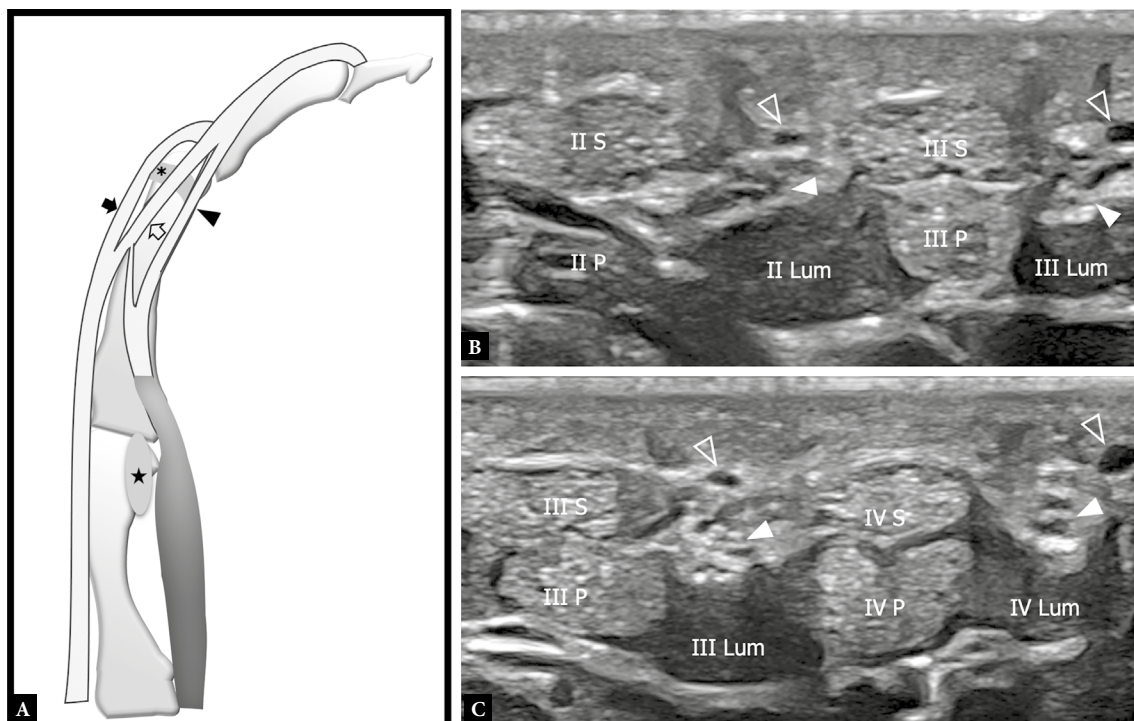


Fig. 7. Lumbrical muscles, normal anatomy. **A.** Schematic drawing demonstrates the relationship of the lumbricals with the deep transverse intermetacarpal ligaments (star) and their distal insertions on the lateral band (outlined arrow), Landsmeer ligament (black arrowhead) and transverse fibers of the extensor hood (asterisk). Black arrow, central band. **B, C.** Short axis 22–8 MHz US images obtained at the level of the distal third of the metacarpals show the position of the second (II Lum), third (III Lum), and fourth (IV Lum) lumbricals in between the tendon slips for the index, middle, and ring finger of the flexor digitorum superficialis (IIS, IIS, and IIS) and flexor digitorum profundus (IIP, IIP, and IIP). Note in (**B**) the unipennate origin of the second lumbrical from the radial side of the tendon slip for the middle of the flexor digitorum profundus and in (**C**) the bipennate origin of the third lumbrical from the ulnar side of the tendon slip for the middle and from the radial side of the tendon slip for the ring. Arrowheads, common digital nerves; outlined arrowheads, common digital arteries

tions respectively on flexor and extensor tendons. The pathomechanism of lumbrical strain has been referred to as the “quadriga effect” and results from the coexistence of opposite forces applied on the muscle belly derived from holding the hand in gripping positions with one or two fingers extended while the adjacent fingers are flexed⁽¹⁶⁾. This position is particularly common in sports like climbing and may expose the lumbricals to a significant biomechanical stress when they have a bipennate origin from two FDP tendons that are alternately relaxed and in tension. This explains why strain

injuries occur most often to the third and fourth lumbricals, which are commonly bipennate. Rest and immobilization have been suggested to be sufficient to treat lumbrical sprain⁽¹⁷⁾. Atrophic changes may be found affecting the first and second lumbricals in median neuropathies and in the third and fourth lumbricals in ulnar neuropathies^(18,19). However, selective atrophy of one lumbrical muscle with sparing of the other muscles may be found in patients with high-grade muscular sprain or traumatic nerve injuries affecting distal motor branches (Fig. 8). Finally, lumbrical intrusion inside

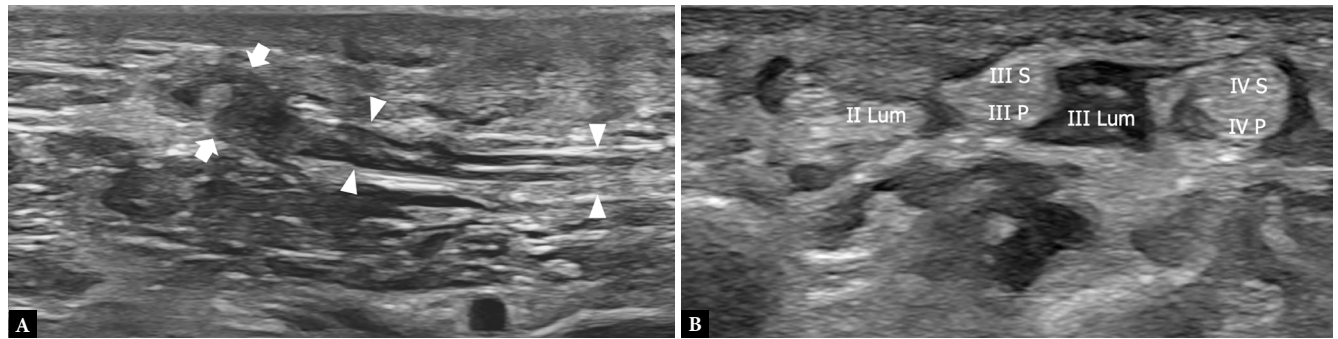


Fig. 8. Selective atrophy of the second lumbrical in a patient with traumatic injury of the first common digital nerve. **A.** Long-axis 22–8 MHz US demonstrates the transected first common digital nerve (arrowheads) ending with a stump neuroma (arrow). **Short-axis axis 22–8 MHz US** shows severe atrophic changes affecting the second lumbrical (II Lum). Note the normal aspect of the third lumbrical muscle (III Lum) which in this patient presents a bipennate origin from the slips of the flexor digitorum profundus for the middle (III P) and ring (IV P) fingers. III S, flexor digitorum superficialis of the middle finger; IV S, flexor digitorum superficialis of the ring finger

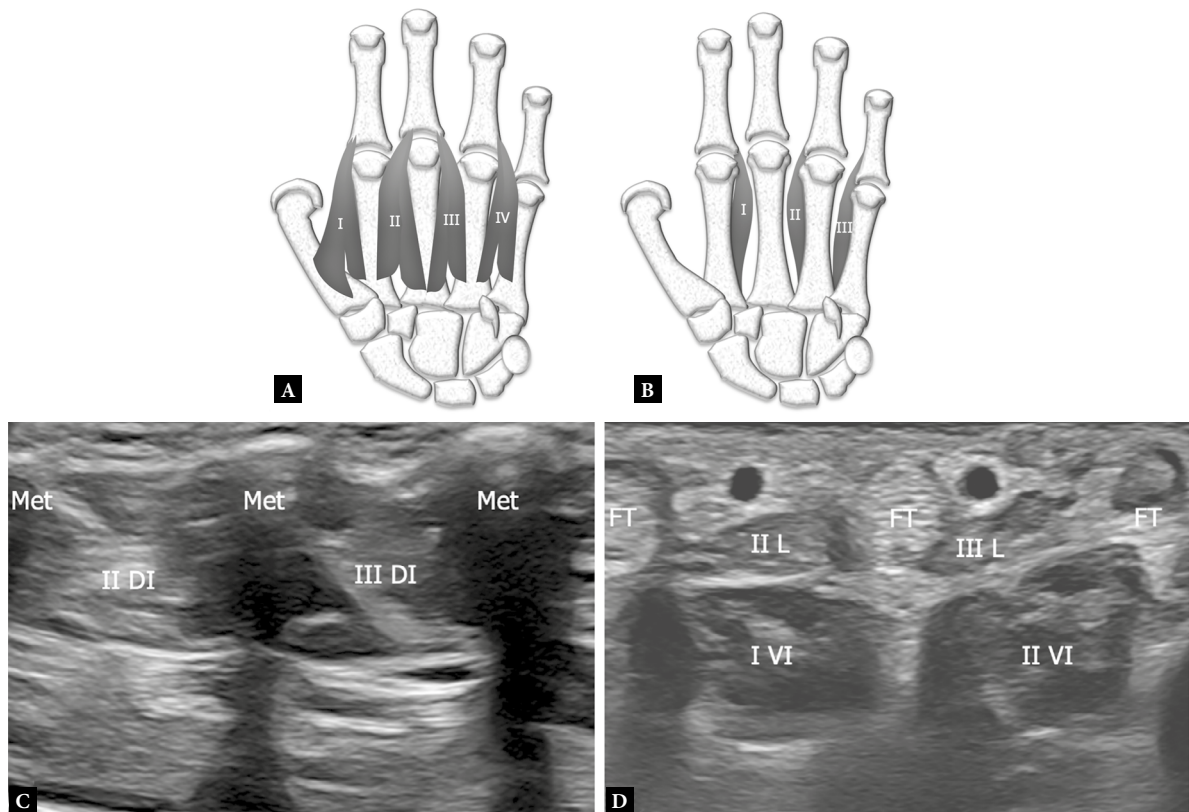


Fig. 9. Dorsal and Ventral Interossei, normal anatomy. **A, B.** Schematic drawings show the proximal and distal insertions of the dorsal and ventral Interossei from the metacarpal shafts and the phalanges, respectively. **C, D.** Short-axis 22–8 MHz US images respectively obtained placing the probe on the dorsal and palmar aspect of the hand at the level of the metacarpal shafts demonstrate the normal appearance of the second (II DI) and third (III DI) dorsal and the first (I VI) and second (II VI) ventral interossei. Met – metacarpal shafts; II L and III L – second and third lumbricals; FT – flexor tendons

the carpal tunnel during flexion of the fingers may contribute to the development of carpal tunnel syndrome in patients with anatomical variants and more proximal origin of these muscles from the flexor digitorum profundus^(20,21).

Ventral and dorsal interossei

The dorsal (DI) and ventral (VI) interossei are seven small muscles located in between the metacarpal shaft and innervated by the deep branch of the ulnar nerve⁽²²⁾. One DI is found in each of the four webspaces of the hand and all of them originate from the corresponding adjacent metacarpal shafts (Fig. 9 A). The first and the second DI respectively insert on the radial side of the index and the middle fingers, whereas the tendons of the third and the fourth reach the ulnar side of the middle and the ring fingers. When considering the distal insertions, however, the variation is more common than the rule. In general, the DI may variably insert into the lateral tubercle of the base of the proximal phalanx, the volar plate, or the extensor hoods. In this latter case, the insertion point is represented by the lateral band, the Landsmeer ligament,

or the transverse fibers. In most instances, the distal tendons insert in both bone and the extensor hood, except for the third DI that more commonly inserts only into the extensor apparatus, and the first DI that in a minority of cases may only have bony insertion. The DI are abductors of the index, middle, and ring fingers and assist the lumbricals in flexing the metacarpophalangeal joints while extending the interphalangeals. Three VI lie in the second, third, and fourth webspace and arise from the ulnar side of the second metacarpal, and the radial sides of the fourth and fifth metacarpals, respectively (Fig. 9 B). The VI insert distally into the proximal phalanges on the same side from which they arise, and their main function is to adduct the index, ring, and little fingers, but they also assist the lumbricals and the DI in flexing the metacarpophalangeal joints while extending the interphalangeals. Like the DI, the VI may insert variably into the lateral tubercle of the proximal phalanx base, the volar plate, the lateral band, the Landsmeer ligament, and the transverse fibers of the extensor hood, but differently from them, most dissection works demonstrated at least some fibers reaching the extensor hood⁽²²⁾. The DI are best appreciated by placing the probe transversely on the dorsal aspect of the hand at the level of the metacarpal shafts, where the muscle bellies are

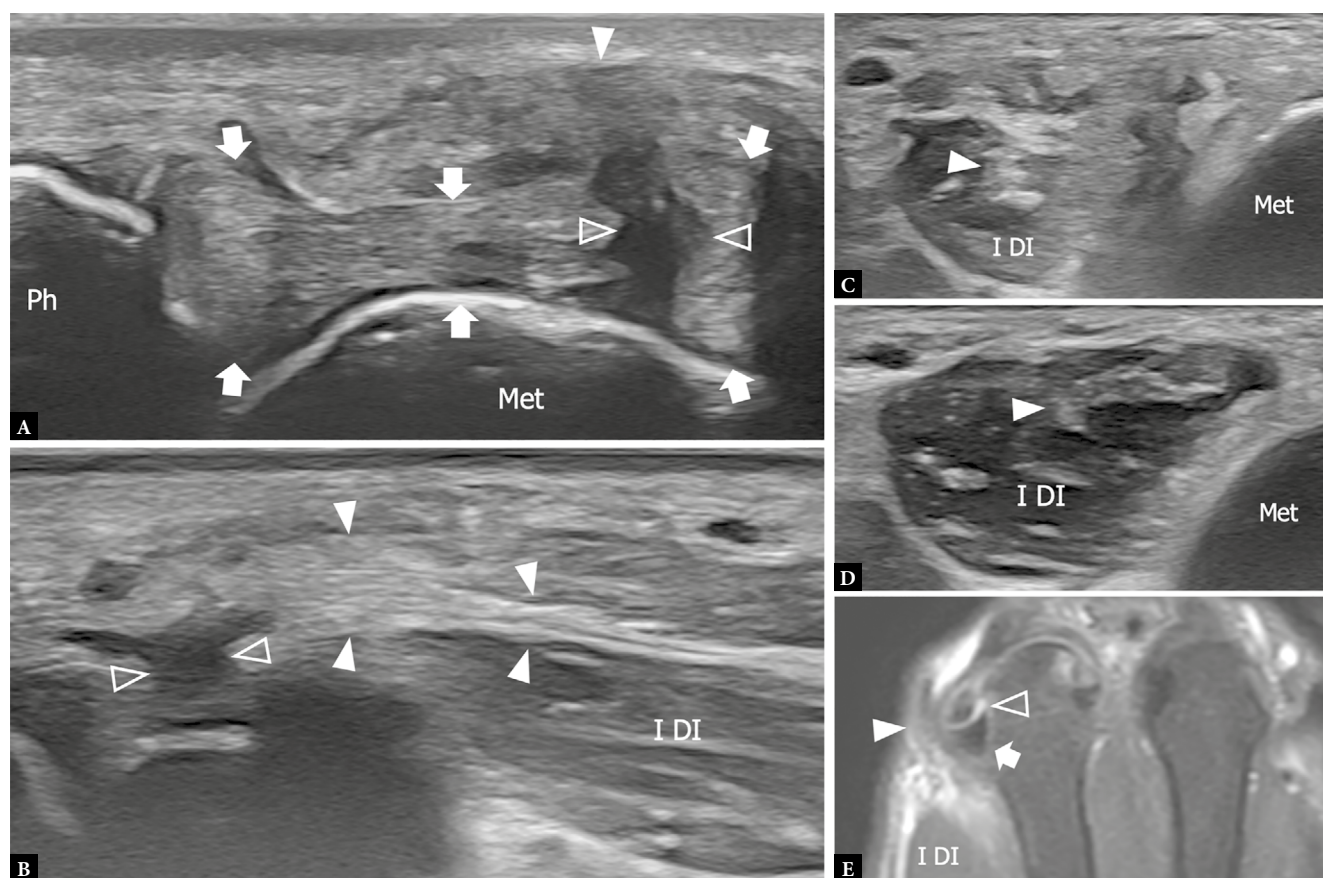


Fig. 10. First dorsal interosseous strain injury in a patient with traumatic full thickness tear of the radial collateral ligament of the second metacarpophalangeal joint. **A, B.** Longitudinal 22–8 MHz US images respectively obtained **A.** at the level and **B.** proximal to the radial aspect of the second metacarpophalangeal joint show severe swelling and inhomogeneous appearance of the preinsertional part (arrowheads) of the distal tendon of the first dorsal interosseous (I DI), in relation to a strain injury. A partial tear (outlined arrowhead) of the deep fibers of the interosseous tendon is demonstrated extending in depth and involving the full thickness of the radial collateral ligament (arrows). **C, D.** Short-axis 22–8 MHz US images of the first dorsal interosseous of the **C** affected and **D.** contralateral hand demonstrate edematous changes with significant hyperechogenicity of the muscle belly associated with mild thickening of the intramuscular aponeurosis (arrowhead). **E.** Coronal STIR MRI confirms the full thickness tear of the ligament (arrow), which shows a hyperintense cleft (outlined arrowhead) in its proximal part. Note moderate edematous changes of the distal tendon of the first dorsal interosseous (arrowhead), which appears thickened and hyperintense

demonstrated occupying each of the four webspaces (Fig. 9 C). Except for the first DI that is easily appreciated along its whole length by means of linear probes, small footprint hokey-stick transducers are required for the evaluation of the distal part of the other DI, as they may be more easily positioned between the metacarpal heads. US evaluation of the VI is performed by placing the probe transversely in the mid palm, where they are appreciated occupying the deep part of the second, third, and fourth webspace underneath the lumbricals and the flexor tendons (Fig. 9 D). Differently from the DI, the distal insertions of the VI are not reliably evaluated with US due to their deep position in a difficult-to-explore area. The interossei can be affected by several conditions, including tenosynovitis typically found in rheumatoid arthritis⁽²³⁾, Dupuytren's disease⁽²⁴⁾, infection⁽²⁵⁾, and trauma⁽²⁶⁾. Even if rare, distraction injuries of distal interossei tendons have been described and may present clinically with pain, tenderness, and impossibility to abduct/adduct the affected finger⁽²⁷⁾. These injuries may be associated with strain of the radial or ulnar collateral ligaments of the metacarpophalangeal joint or distraction of the lumbrical tendons and may require surgical repair to correct finger deformity and function. US can recognize distraction injuries of the interossei, distinguish low-grade muscle strain from tendon avulsion, and identify the associated lesions involving the locoregional structures (Fig. 10).

References

1. Nemoto K: Restoration of the first dorsal interosseous muscle by transfer of the abductor pollicis longus tendon. *Scand J Plast Reconstr Surg Hand Surg* 2002; 36(4): 249–252. doi: 10.1080/02844310260259969.
2. Klein CS, Liu H, Zhao CN, Yang X: Quantitative ultrasound imaging of intrinsic hand muscles after traumatic cervical spinal cord injury. *Spinal Cord* 2021; 60(3): 199–209. doi: 10.1038/s41393-021-00653-1.
3. Gupta S, Michelsen-Jost H: Anatomy and function of the thenar muscles. *Hand Clin* 2012; 28(1): 1–7. doi: 10.1016/j.hcl.2011.09.006.
4. Fernandes CH, Meirelles LM, Raduan Neto J, Nakachima LR, Dos Santos JB, Faloppa F: Carpal tunnel syndrome with thenar atrophy: evaluation of the pinch and grip strength in patients undergoing surgical treatment. *Hand (N Y)* 2013; 8(1): 60–63. doi: 10.1007/s11552-012-9471-8.
5. Eisen A, Kuwabara S: The split hand syndrome in amyotrophic lateral sclerosis. *J Neurol Neurosurg Psychiatry* 2012; 83(4): 399–403. doi: 10.1136/jnnp-2011-301456.
6. Nguyen JT, Nguyen JL, Wheatley MJ, Nguyen TA: Closed traumatic rupture of the thenar muscles from the origin: a case report and review of the literature. *Ann Plast Surg* 2015; 74(3): 300–303. doi: 10.1097/sap.0b013e3182996ec4.
7. Ganguly A, Chaudhary SR, Rai M, Kesavanarayanan V, Aniq H: Thenar lumps: a review of differentials. *Clin Radiol* 2019; 74(12): 978.e15–978.e27. doi: 10.1016/j.crad.2019.08.025.
8. Jacobson JA, Middleton WD, Allison SJ, Dahiya N, Lee KS, Levine BD: Ultrasonography of superficial soft-tissue masses: Society of Radiologists in Ultrasound Consensus Conference Statement. *Radiology* 2022; 304(1): 18–30. doi: 10.1148/radiol.211101.
9. Pasquella JA, Levine P: Anatomy and function of the hypothenar muscles. *Hand Clin* 2012; 28(1): 19–25. doi: 10.1016/j.hcl.2011.09.003.
10. Murata K, Tamai M, Gupta A: Anatomic study of variations of hypothenar muscles and arborization patterns of the ulnar nerve in the hand. *J Hand Surg* 2004; 29(3): 500–509. doi: 10.1016/j.jhsa.2004.01.006.
11. Moore CW, Rice CL: Structural and functional anatomy of the palmaris brevis: grasping for answers. *J Anat* 2017; 231(6): 939–946. doi: 10.1111/joa.12675.
12. Dy CJ, Mackinnon SE: Ulnar neuropathy: Evaluation and management. *Curr Rev Musculoskelet Med* 2016; 9(2): 178–184. doi: 10.1007/s12178-016-9327-x.
13. Atkins SE, Logan B, McGrouther DA: The deep (motor) branch of the ulnar nerve: a detailed examination of its course and the clinical significance of its damage. *J Hand Surg Eur Vol* 2009; 34(1): 47–57. doi: 10.1177/1753193408097489.
14. Yuen JC, Wright E, Johnson LA, Culp WC: Hypothenar hammer syndrome: an update with algorithms for diagnosis and treatment. *Ann Plast Surg* 2011; 67(4): 429–438. doi: 10.1097/sap.0b013e31820859e1.

Conclusion

High-resolution US represents the first line imaging modality to investigate pathologies involving the intrinsic muscles of the hand and may provide diagnostic information that significantly impacts therapeutic decisions. Knowledge of regional anatomy and hand biomechanics is an essential prerequisite to performing a targeted exam and enhancing the diagnostic potential of this modality.

Conflict of interest

The authors do not report any financial or personal connections with other persons or organizations which might negatively affect the contents of this publication and/or claim authorship rights to this publication.

Author contributions

Original concept of study: RP, FZ, CM. Writing of manuscript: RP, FZ, FP, CM. Analysis and interpretation of data: RP, FZ, MMP, MM, DB, CM. Final approval of manuscript: RP, FP, CM. Collection, recording and/or compilation of data: RP, SR, MP, GR, LT, CM. Critical review of manuscript: CM.